Progress In Electromagnetics Research, PIER 59, 151–174, 2006

PREDICTION OF PROPAGATION CHARACTERISTICS IN INDOOR RADIO COMMUNICATION ENVIRONMENTS

N. Yarkoni and N. Blaunstein

Department of Communication Systems Engineering
Ben-Gurion University of the Negev
Beer Sheva, Israel

Abstract—In this work, we present a semi empirical approach and the analytical model on how to predict the total path loss in various indoor communication links, taking into account the new analytical methods of the derivation of the fading phenomenon between floors and along corridors, respectively. We take into account the stochastic method of slow and fast fading estimations, caused by diffraction and multipath phenomena, respectively. The statistical parameters required for statistical description of the diffraction and multipath phenomena, such as the standard deviations of the signal strength due to slow and fast fading are obtained from the corresponding measurements. The path loss characteristics together with evaluated parameters of slow and fast fading give a more precise link budget predictor, and obtain full radio coverage of all subscribers located in the area of service inside each building. Based on strict and completed path loss prediction, an algorithm of link budget performance is presented for different scenarios of radio propagation within indoor communication links. Results of proposed unified approach are compared with the analytical Bertoni's model, which is well-known and usually used in link budget design in various indoor environments. The results are also compared with measurements carried out for different propagation scenarios, along corridor and between floors, occurred in the indoor communication channels. A better agreement with experimental data is obtained compared to the model in consideration.

1. INTRODUCTION

The increasing demand for indoor wireless applications, such as wireless LAN, "Smart house", etc., creates a need to efficiency and performance. While designing an indoor wireless systems one is required to place the picocell antennas (at ranges that do not exceed 100 m, see definitions of types of cells in [1–4]) in a way that will provide an optimal coverage of the building area. There are many scenarios for the indoor wireless communication, starting from communication between two stationary antennas, to communication between a moving antenna, such as a person walking along a street, and a stationary antenna. The indoor wireless propagation scenarios can be divided into two scenarios. The first is when one antenna is located outside a building and the other is inside it [5–7]. The main reason for the measurements in this category is to give an answer to the broadening of the current wireless services to indoor application of both types of services. The second scenario in when both antennas are located inside the building [8–11]. The motivation to research this category is the establishment of specialized indoor communication systems. Although the impulse response approach is compatible with both, it has been mainly used for measurements and modeling effort reported in the second category.

Investigators have tried to compute and to determine a radio coverage that will predict a suitable antenna spanning for each building characteristics and wireless system requirements. There are many models, developed in recent decades, which describe the propagation of signals in space [12–23]. The ability to predict the behavior of signals in indoor environments is crucial. The full understanding of these models and their unification to a more applicable one will allow a better behavioral prediction and better capabilities in the design of indoor communication networks. The indoor radio propagation environment is specified by many features and characteristics and is very complex [1, 3, 4]. Adding all these variables together forms a great problem. Due to this fact, dealing with these characteristics and with different propagation models, used to calculate them, has to be done efficiently and accurately.

Every indoor communication system has a different structure and requirements due to their various applications. Therefore giving an accurate answer to each indoor communication system using the same models is a complex task. Calculating path loss for an indoor environment is difficult. Because of the variety of physical barriers and materials within the indoor structure, one cannot exactly predict the loss of signal energy. Obstacles such as walls, ceilings and furniture,

usually block the path between receiver and transmitter. Depending on the building construction and layout, the signal usually propagates along corridors and into other open areas. In some cases, transmitted signals may have a Line-of-Site (LOS) to the receiver. In most cases a non-line-of-sight (NLOS) conditions i.e., the signal path is obstructed. Finally, those who are involved in the wireless discipline whether as a designer or a user, must be aware of the interiors and exteriors construction materials, and of the obstructions locations of a building to best position wireless equipment. For optimal performance the user should also consider work activities.

The multipath dispersion in an indoor channel is caused by a large number of reflectors and scatterers. The indoor channel is not stationary both in space and in time domains. The motion of people and equipment around the low-level portable antennas cause temporal variations in the indoor channel statistics. Furthermore, the indoor channel is characterized by higher path losses and sharper changes in the mean signal level, as compared to the mobile channel [3, 24, 25]. At the same time, the Doppler shift effects in the indoor channel are negligible, because the indoor environment lacks the rapid motions and high velocities, typical to the mobile users. The indoor channel is characterized by excess delays of less than one μs, and rms delay spread of several tens to several hundreds of nanoseconds (most often less than 100 ns [3, 26]). Finally, the indoor wireless channel differs from the outdoor channel in two main aspects, the environment is much variable relative to the path length, and the coverage size is smaller

Moreover, in real life situation of indoor propagation environment, multipath occurs when there is more than one path available for radio signal propagation. The reflection, diffraction and scattering phenomena cause additional radio propagation paths to the direct LOS path between the transmitter and receiver. Much the same as outdoor environment, we use attenuation or path loss, the fast and slow fading [1–23] in order to describe all these phenomena. At the same time, construction materials of the building and the building type influence propagation inside buildings.

Indoor radio propagation is ruled by multiple reflection, diffraction and scattering from natural and man-made obstructions in the indoor channel. However, the circumstances vary much more than in outdoor environments (see [1–4]). The received signals of an antenna mounted on a desk at an open space office with partitions are very different from those received at an antenna mounted on the outdoor propagation links. The small propagation distances make it more difficult to insure far-field radiation for all the receiver locations and types of antennas.

Partitions are amongst the main indoor signals' losses reasons, they occur when terminal antennas are assembled at the same floor, and losses between floors occur when terminals are in clutter (NLOS) conditions

Obviously, as in outdoor propagation channels, there is not a unified theoretical model for path loss and fading effects prediction in indoor communications [1–4]. For each scenario of the indoor environment (propagation along corridors, inside a room and between floors and walls) the corresponding model is usually used.

In our work we present a semi-empirical model which is based on more precise evaluation of fading phenomena, slow and fast. This model use a statistical description of the channel [2], where the main parameters of slow and fast fading are obtained from the corresponding measurements both in conditions of line-of-sight (LOS) and non-line-of-sight (NLOS) when radio signal passes several floors and walls. The model is compared with Bertoni's analytical model [1], from which we take information about path loss between floors combined with statistical approach [2] for fading effects estimation for total link budget performance. As for propagation along corridor, a new analytical waveguide model is performed based on [33] and compared with the corresponding experiments. In such scenario, comparison of the proposed model with the corresponding measurements is also presented. A better agreement with experimental data is obtained compared to the Bertoni's analytical model for propagation between floors in NLOS conditions, and a good agreement with the experimental data for the scenario of propagation along corridors in LOS conditions is also obtained.

2. RADIO PROPAGATION IN INDOOR ENVIRONMENT: THEORY AND MODELS

2.1. Modeling of Loss Characteristics in Various Indoor Environments

This section briefly outlines models for path loss within buildings, including the proposed semi empirical model. We focus on the propagation models most used in practical application and will show our approach to the problem of loss characteristics prediction in different indoor communication links through the prism of the corresponding experiments.

2.1.1. Physical Waveguide Model of Radio Propagation along the Corridor

We propose an analytic model of radio wave propagation along impedance corridor as unbroken waveguide. The same model was successfully approbated for outdoor communication scenario consisting straight crossing street waveguides [2]. The proposed waveguide model, which differs from existing models [14, 18], allow us to analyze the electromagnetic fields distribution inside the corridor and finally to obtain an expression for the attenuation (extinction) length and the path loss.

The Geometry of the Problem. Below we briefly present the guiding effects of the corridor based on the same theoretical approach as was done for the outdoor street scene [2], that is, we model the corridor using the two dimension (2-D) impedance parallel waveguide (Fig. 1).

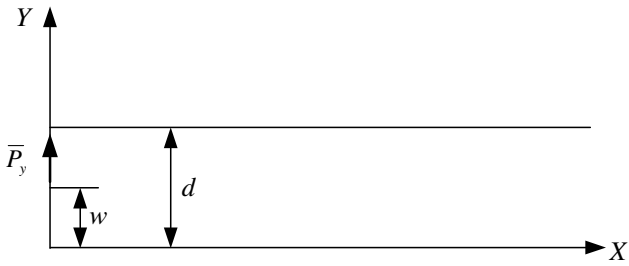

Figure 1. The waveguide model of corridor; a view from the top.

Because $d \gg \lambda$, where d is the corridor's width and λ is the wavelength, we can use the approximation of geometrical theory of diffraction (UTD). This approximation is valid as long as the first Fresnel zone $\sim (\lambda x)^{1/2}$, equals or does not exceed the width of corridor d. In this case, $x \leq$ 30–50 m, λ =3–10 cm (L/X-band); d =2–3 m; $(\lambda x)^{1/2} \leq d$.

The electrical properties of walls are defined by surface impedance $Z_{TE} \sim \varepsilon^{-1/2}$, $\varepsilon = \varepsilon_0 - j(4\pi\sigma/\omega)$, where ε is the dielectric permittivity of the wall's surface, ε_0 is the dielectric constant of the vacuum, σ is the conductivity, and $\omega = 2\pi f$ is the angular frequency of the radiated wave.

We consider the 2-D problem of wave reflection without taking into account the reflection from the corridor's floor and ceiling, because the corridor's height H and the position of the transmitter/receiver h =2–3 m, are usually larger values than λ. Let us also assume, according to

geometry presented in Fig. 2, that a vertical electric dipole is placed at the point $(0, w, h)$ at the (y, z)-plane, as it is shown in Fig. 3.

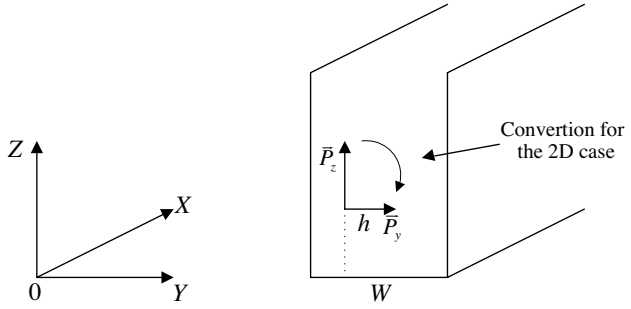

Figure 2. The corridor in the 2-D case.

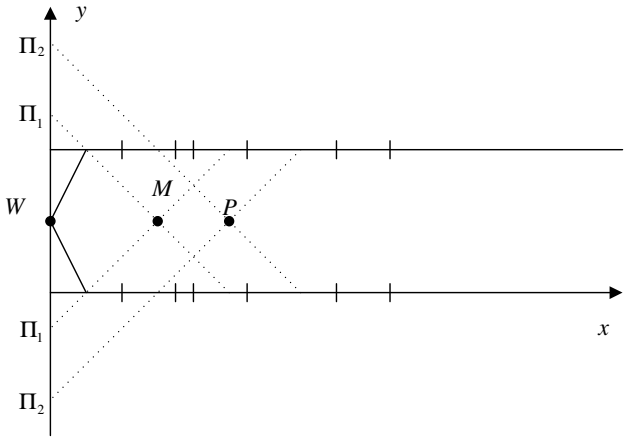

Figure 3. The waveguide modes created by the corresponding image sources.

To revert the problem to a 2-D case, we must consider the dipole oriented along the y-axis, that is, the horizontal dipole with respect to the (x, y)-plane, which corresponds to the well-known electromagnetic field equation described by the Hertzian potential vector $\Pi_y^i(x, y)$ [33]:

$$\nabla^2 \Pi_y^i(x, y) - k^2 \Pi_y^i(x, y) = \frac{4\pi i}{\omega} \mathbf{p}_y \delta(x)\delta(y - w) \tag{1}$$

The solution of such an equation can be presented using Green's

function [2]:

$$\Pi_y^i(x,y) = \frac{i}{\omega}\mathbf{p}_y \frac{e^{ik\rho}}{\rho} \tag{2}$$

Here $\mathbf{p}_y$ is the electric momentum of a point horizontal electric dipole, $\rho = \sqrt{x^2+y^2}$ is the distance from the source.

Total Field in 2-D Unbroken Impedance Waveguide. The reflected field in an unbroken waveguide can be determined according to [33] as a sum of reflected modes replaced by the image sources (as shown in Fig. 3).

The straight computations made according to [33] finally give the normal mode expression inside the impedance waveguide (called the *discrete spectrum* of the total field):

$$\Pi_n(x) = D_1 e^{i\rho_n^{(0)}x} \exp\left\{-\frac{|\ln|R_n||}{\rho_n^{(0)}d}\left(\frac{\pi n}{d}\right)x\right\} \tag{3}$$

where $\rho_n^{(0)} = \sqrt{k^2 - K_n^2} = \sqrt{k^2 - \left(\frac{n\pi}{d}\right)^2}$ and $R_n = \frac{K_n - kZ_{EM}}{K_n + kZ_{EM}}$; $D_1 = \frac{2DR_n}{i\rho_n^{(0)}d}$; $K_n = \frac{n\pi}{d}$ is the wavenumber of normal modes of number n that propagate along the waveguide with width d, $k = \frac{2\pi}{\lambda}$, $D = -(4\pi i/\omega)|\vec{\mathbf{p}}_y|$, $\vec{\mathbf{p}}_y$ is the electric momentum of a point horizontal electric dipole, $\omega = 2\pi f$.

Following [33], we also can present the continuous spectrum of total field for $x/d \gg 1$ as:

$$\Pi_e \approx \sqrt{2}De^{i\left(\frac{3\pi}{4}\right)}\frac{1-|R_n|}{1+|R_n|}\frac{e^{ikx}}{x} \tag{4}$$

For the case of perfectly conductive waveguide, when $|R_n| = 1$, $Z_{EM} = 0$, we obtain that $\Pi_c = 0$, that is, in the case of the ideal conductive waveguide, the continuous part Π_c of the total field vanishes for this large distances ($x > d$), and only the discrete spectrum of the normal waves propagates along the ideal waveguide without attenuation according to (3). Finally, the intensity of the total field can be approximately obtained as:

$$I \approx \lfloor(\Pi_n + \Pi_e)\cdot(\Pi_n + \Pi_e)^*\rfloor$$

The path loss of radio wave can be derived as:

$$\begin{aligned} L \approx\ & 32.1 - 20\log_{10}|R_n| - 20\log_{10}\left[\frac{1-[R_n]^2}{1+|R_n|^2}\right] + 17.8\log_{10}x \\ & +8.6\left\{-[\ln|R_n|]\left(\frac{\pi n}{d}\right)\frac{x}{\rho_n^{(0)}d}\right\} \end{aligned} \tag{5}$$

where x is the distance between two terminals, receiver and transmitter along the corridor.

Simulation and Analysis of the Waveguide Corridor Model. Let us present some examples of simulation of the total path loss L in decibels (dB) according to (5) versus distance between the transmitter and receiver. For the numerical computations, we took: the width of the corridor $d = 3\,\mathrm{m}$, the conductivity of walls $\sigma = 0.0133\,\mathrm{S/m}$; the signal frequency $f = 900\,\mathrm{MHz}$. The result of our computations of the path loss according to (5) is shown in Fig. 4 for the guiding modes with number n of 1 to 10.

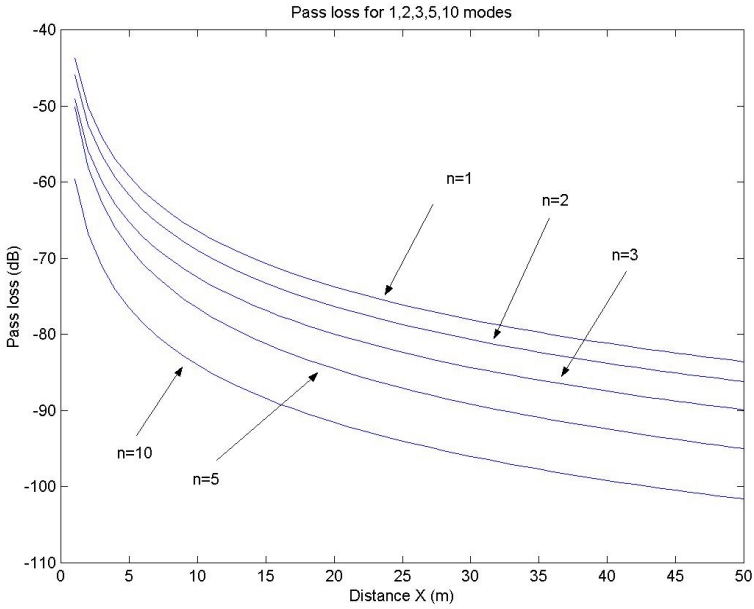

Figure 4. Path loss for two first modes versus distance from the transmitter.

As seen from the presented computations for $n \geq 3$, the effect of these modes is negligible at ranges beyond 20 meter. We just have to subtract the attenuation from the first two main modes of the original signal power in order to get the total power of a signal (in dB) for each distance d between the transmitter and the receiver located along the corridor waveguide. The same effect was also shown in [33] for outdoor communication links consisting channels with streets guiding structure, where it was obtained experimentally that the only one-two main modes are important at the ranges of ten and more meter

from the transmitter. Figure 4 stresses the same effect, but for indoor communication link in LOS conditions.

2.1.2. Physical Model of Radio Propagation between Floors and Walls

Bertoni with colleagues have developed a theoretical model, based on the geometrical theory of diffraction (GTD), which explains the propagation between a transmitter and a receiver located on different floors of a building [1, 21, 22]. Depending on the structure of the building and the location of antennas, either direct ray propagation through floors or diffraction outside the building will determine the propagation characteristics and range dependence of the signal. There are two paths over which propagation can take place:

1) Paths that runs through floors.
2) Paths that have segments outside the building and involve diffraction caused by the window frames.

The paths through the floors include the direct ray path and the rays that are multiply reflected and transmitted at semi-transparent walls and floors. These rays are contained entirely within the building perimeter. The diffracted ray paths involve transmission outside the building through windows and diffraction into paths that run along side the face of the building and than reenters through another window at a different floor. For the propagation of the direct ray through semitransparent floors, as indicated by path T in Fig. 5, according to [1], the electromagnetic field strength in general reaching a receiving site is given by [21, 22]

$$|\mathbf{E}|^2 = \frac{Z_0 P_e}{4\pi L^2} \prod_m T_{floor,m}^2 \prod_n T_{wall,n}^2 \tag{6}$$

Here Z_0 is the free space wave impedance $= 120\pi\Omega \sim 377\Omega$, P_e is the effective transmitted power and L is the direct distance between the transmitter (Tx) and the receiver (Rx) antennas. T_{floor} and T_{wall} are the loss coefficients of each floor and wall, respectively, passed by the direct ray. Such a direct ray, passing through three floors and two interior walls, is indicated in Fig. 5. If one knows the reflection coefficient Γ of each wall and floor, than we can calculate T_{floor} or T_{wall} as [21, 22]:

$$T = \sqrt{X\left(1 - |\Gamma|^2\right)} \tag{7}$$

where X is a constant, obtaining from the concrete experiment. The signal can also reach other floors via paths that involve diffraction.

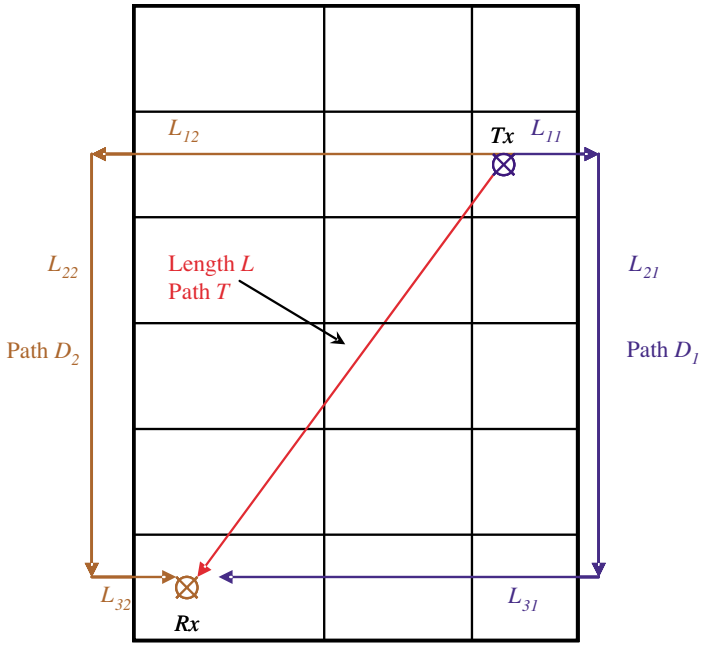

Figure 5. Scheme of the Bertoni's model [1].

Referring to paths D_1 and D_2 in Fig. 5 (in general denoted as D_i), the field reaching the receiver via one such diffracted path is given by [21, 22]:

$$|\mathbf{E}|^2 = \frac{Z_0 P_e}{4\pi} \frac{\prod_i D^2(\alpha_i) \prod_j T^2_{glass,j} \prod_k T^2_{wall,k}}{\prod_m \sum_n L_{nm}} \tag{8}$$

where L_{nm} is the length of D_i diffracted path. In the geometry of the concrete experiment carried out in the hotel schematically presented in Fig. 5 according to [1], L_{nm} is the length of D_1 and D_2 where $\prod_m \sum_n L_{nm} = (L_{11}+L_{21}+L_{31})(L_{12}+L_{22}+L_{32})$, $T_{glass(m)}$ and $T_{wall(n)}$ are the transmission coefficients through glass and through interior walls crossed by path segments. In (8) $D(\alpha_i)$is the diffraction coefficient for a propagating ray bending through angle α_i. Depending on the construction of the building and window frame, different choices may be made for the diffraction coefficient. For simplicity in investigating the relative strength of the total field associated with the direct ray and the diffracted ray, the coefficient for an absorbing wedge obtained

by Keller's diffraction theory [1], was used:

$$D(\alpha_i) = \frac{1}{2\pi k}\left[\frac{1}{2\pi + \alpha_i} - \frac{1}{\alpha_i}\right] \tag{9}$$

where $k = 2\pi/\lambda$ is the wave number. Thus, when propagation takes place through the floors, the signal will decrease rapidly with the number of floors separating the transmitter and the receiver. On the other hand, if propagation occurs via diffracted paths, the signal will be small even for separation by a single floor, but will decrease more slowly with increased separation.

For testing the model an experiment was made according to Fig. 5 in the frequency of 852 MHz where according to presented geometry the angle $\alpha_i = \pi/2$. Measurements have shown that in each floor attenuation was about 12–13 dB. From experiments and the knowledge of material, coefficients of walls floors and windows for the specified building were defined in dB as

$$T_{wall} = 2.2\,\text{dB}: \quad T_{glass} = 0.25\,\text{dB}: \quad T_{floor} = 13.0\,\text{dB} \tag{10}$$

Total received power in dB at Rx position can be calculated according to (6) for the direct path through floors and walls

$$P_{r\,Direct} = 10\log_{10}\lambda^2|E|^2_{direct}\Big/(Z_0 \cdot 4\pi)\ [\text{dB}] \tag{11}$$

where $P_{r\,Direct}$ is the power gain from direct propagation wave, $|E|^2$ is calculated according to (6) and $\lambda = \frac{c}{f}$ is the wavelength. Then, according to the same relation, as (11), we get:

$$P_{r\,Diff} = 10\log_{10}\lambda^2|E|^2_{diff}\Big/(Z_0 \cdot 4\pi)\ [\text{dB}] \tag{12}$$

where $P_{r\,Diff}$ is the power gain from diffracted propagation wave, $|E|^2$ is calculated according to (8). Then the total received power will be:

$$P_{r\,total} = P_{r\,Direct} + P_{r\,Diff}\ [\text{dB}] \tag{13}$$

Deep analysis of Bertoni's model and comparison with numerous experiments carried also by authors of this work (see below Section 3) have shown that despite the fact that this model offers complete physical calculations, which are suitable for different kind of buildings, the attenuation effects due to shadowing caused by diffraction from internal obstructions are not taking correctly in consideration. As will be shown below, this type of attenuation must be accounted, because it can decrease the total strength of radio signal that reaches the receiver by 10 to 15 dB.

However, the shadow effect is concrete only at the upper floors that is, when difference between antenna locations is more than two-three floors; for the location of both terminal antennas at the bottom floors the shadowing effects are not so actual. Additional analysis has shown that the software implementation of Bertoni's model is not so simple; it needs previous knowledge of precise building architecture and establishing of variable paths of wave propagation, which by all means is very difficult. Most of the buildings differ by structure, thus it is inevitable to calculate the diffracted paths according to sketches (no software involved), and may come in great inaccuracy and a waste of great deal of time. At the same time, estimation of path loss through walls and floors according to (6) is most precise procedure compared to other existing empirical models (see formulas (14) and (15) below). Therefore we will use (11) in the proposed unified approach for link budget design in indoor communication links taking into account both shadowing (slow fading) and multipath (fast fading) effects caused by internal obstructions located within the radio path connected terminal antennas.

2.1.3. Empirical Models

Such models are based mostly on numerous experiments carried out in various indoor environments as a best-fit prediction to the corresponding measured data.

Rappaport's Path Loss Prediction Model. Rappaport and his associates [3, 11, 13, 20] made a lot of experiments in various indoor environments in different locations and sites. The main goal of these experiments was to achieve unique parameters of attenuation and loss prediction on different kind of multi-floored buildings.

Distance-Dependent Path Loss Model. In [3, 20] was assumed that the mean path loss $\overline{L}$ is an exponential function of distance d with the power n:

$$\overline{L}(d) \propto \left(\frac{d}{d_0}\right)^n \tag{14}$$

where $\overline{L}(d)$ is mean path loss, n is the mean path loss exponent which indicates how fast path loss increases with distance, d_0 is a reference distance, usually is chosen to equal 1 meter in indoor communication links, and d is the transmitter receiver separator distance. Absolute mean path loss, in dB, is defined as the path loss from the transmitter to the reference distance d_0, plus the additional path loss [3], that is,

$$\overline{L}(d) = L(d_0) + 10 \cdot n \cdot \log\left(\frac{d}{d_0}\right) \text{ [dB]} \tag{15}$$

For these data, $L(d_0)$ is the reference path loss due to free space propagation from the transmitter to a 1 m reference distance, and calculated by:

$$L(d_0) = 20 \log \left(\frac{4\pi d_0}{\lambda} \right) \text{ [dB]} \tag{16}$$

The proposed model empirical model takes into account effects of shadowing by introducing in (15) a term X_σ, which describes statistical character of slow fading within the indoor link and as a random variable satisfies the log-normal distribution with a standard deviation of σ in dB. Then the total path loss within building equals in dB [3]:

$$L(d) = L(d_0) + 10 \cdot n \cdot \log \left(\frac{d}{d_0} \right) + X_\sigma \text{ [dB]} \tag{17}$$

For this model the exponent n and standard deviation σ were determined as parameters which are functions of building type, building wing, and number of floors between Tx and Rx. Thus a model to predict the path loss for a given environment is given by [3]

$$L(d) = \overline{L}(d) + X_\sigma \text{ [dB]} \tag{18}$$

where X_σ is a zero mean log-normally distributed random variable with standard deviation σ and accounts for attenuation due to diffraction from environment characteristics. Detailed analysis of the Rappaport's model has shown that there are some difficulties to use this model in practical applications for indoor environments. Rappaport's model offers an estimation accuracy of indoor path loss prediction and retrieves its main parameters through experiments, that is, to achieve a precise estimation of a desired building one must perform many experiments in that building and achieve all parameters through the offered model. However, there is no some actual predicting model for a specific building. Only estimation exists according to experiments.

Let us now compare two approaches, Bertoni and Rappaport, through the experimental data. The Rappaport's model based on experimental factors, and it does not provide the radiowave propagation characteristic such as the attenuation inside buildings in situations when the transmitter and the receiver are located at the different floors. Moreover, the Rappaport's model based on experimental parameters and it does not provide any characterization of the path loss between floors.

According to Bertoni's model we *a-priori* know that in the upper floors of the building the attenuation is sharply changed due to the additional loss that occurs due to the diffraction path through the

windows according to (13). At the same time, Rappaport's model does not provide the investigator any information about it, so we need information about measurements at every floor. Also the slow fading effect, called shadowing [1–4], can be easily represented in the Bertoni's model, as the additional effect of the wave field that comes from the diffraction paths. Therefore, the Rappaport's model should be used in cases where only buildings with a low number of floors (up to two floors) exist. It is very similar to the Bertoni's model in the lower floors when radio propagation is mostly occurs through the direct path and described by (6). When higher buildings are tested, the Bertoni's model, as more appropriate model, should be used with additional improvements by accounting fading effects, as will be presented below. Furthermore, in his empirical model (15)–(17), Rappaport used a term X_σ which was evaluated from special experiments that take into account only the effects of floors [3]. Rappaport doesn't take into account effects of corners, walls and windows, as was done by Bertoni [1], and what we use in our modified model following [2]. According to those reasons, we do not compare our modified semi-empirical model to the Rappaport's model when buildings with more than two floors are tested.

2.1.4. Suggested Model

In the suggested model for the radio propagation between floors, we take into consideration the physical media and parameters of total path loss obtained from experiments. In general the suggested model will follow the formula:

$$L_{total} = \overline{L} + L_{fading} \text{ [dB]} \tag{19}$$

which is similar to (18) as shown in the Rappaport's model, only now $\overline{L}$ is the loss achieved from a direct propagated ray with NLOS features and

$$L_{fading} = L_{SF} + L_{FF} \tag{20}$$

Here $L_{SF} = 10 \log \sigma_{SF}$, where σ_{SF} is a zero mean log-normal distributed random variable with standard deviation σ_L in dB, and accounts for attenuation from diffracted propagated waves (so called the shadowing effect from obstructions). $L_{FF} = 10 \log \sigma_{FF}$, σ_{FF} is the Ricean distributed random variable with standard deviation σ in dB, and accounts for multipath (multiple reflections and scattering) phenomena caused by obstructions located surrounding the terminal antennas. It can be obtained from experiments, which were made in different building environments (see full algorithm in [2] on how to

obtain link budget for outdoor and indoor communication links). Let us briefly present this algorithm.

Estimations of shadowing effects. At this step, we obtain the standard deviation of *slow fading*, σ_L, as a logarithm of ratio between the signal strength with and without diffraction phenomena, obtained experimentally, which give main influence on shadowing from building contours. Finally, this allows us to obtain the fade margin using algorithm described in [2] taking into account shadowing effect from building roofs and corners:

$$\sigma_{SF} = 2\sigma_L \text{ and } L_{SF} = 10\log\sigma_{SF} \tag{21}$$

Estimations of multipath effects. To obtain information about the *fast fading margin*, L_{FF}, we need, first of all, the knowledge of the Rician parameter K as a ratio of coherent (LOS component) and incoherent (multipath component without diffraction) parts of the total signal intensity [2], i.e.,

$$K = \frac{\langle I_{co}\rangle}{\langle I_{inc}\rangle} \tag{22}$$

Then, we use the corresponding formula of Rician distribution, which allows us to obtain σ_{FF} or L_{FF} using well-known equation:

$$\begin{aligned} L_{FF} &= 10\log\sigma_{FF} \\ &= 10\log\left\{\int_0^\infty x^2 PDF(x)dx - \left(\int_0^\infty xPDF(x)dx\right)^2\right\} \text{ dB} \end{aligned} \tag{23}$$

where x is the random amplitude of the received signal, $PDF(x)$ is the corresponding probability density function. Using (23) we get [2]:

$$\begin{aligned} \sigma_{FF} &= \left[2\cdot(rms)^2\cdot e^{-K}\right]\cdot\left[\frac{1}{2}\cdot e^K\int_0^\infty y^3\cdot e^{-y^2}\cdot I_0\left(2\cdot\sqrt{K}\cdot y\right)\cdot dy\right. \\ &\quad \left. -\left(\int_0^\infty y^2\cdot e^{-y^2}\cdot I_0\left(2\cdot\sqrt{K}\cdot y\right)\cdot dy\right)^2\right]^{1/2} \end{aligned} \tag{24}$$

Here, rms is the root mean square of the random amplitude x, $I_0(w)$ is the zero order Bessel function of variable w.

The average path loss between floors $\overline{L}$ must be calculated according to the direct NLOS attenuation described by (6) following the Bertoni's model. In the other words, model (19) is combination of

the Bertoni's physical model of direct propagation through floors (6) and statistical approach, proposed in [2] for outdoor link budget design, by estimation of the parameter L_{fading} from (20) using experimental data for σ_L, σ and K estimation.

The proposed path loss model is based on two essential aspects. First, it uses Bertoni's prediction to obtain the received power signal along the radio path of rays penetrated through floors and described by (6) and second, it uses our statistical measured σ_L, σ, K and the method of fade margin estimation according to procedure of link budget design described in [2]. Such approach is easy to calculate mathematically with simple software implementation and simulation.

3. LINK BUDGET DESIGN VERIFICATION VIA EXPERIMENTAL DATA

In order to investigate the accuracy of the well-known models and the suggested above models of radio propagation along the corridor (5) and between floors and walls described by (19) with help of (20)–(23) for the path loss evaluation, we carried out some special experiments within several four-storied campuses of Ben-Gurion University (Israel). The main goal of such experiments is a special test of the measured data compared to each suggested model and the final proposition on how to design a link budget and to obtain radio coverage for each experimental site. Based on simulation and experiments we can establish whether the model that is suggested fits the results and can be recommended for further applications.

Path Loss Along the Corridor. The system consists of 2 main parts. The first is a wireless accesses point connected to a power supply and the second is a laptop with a corresponding wireless LAN card. The laptop was located on a portable surface in order to separate it from the floor. The LAN card and the accesses point ware initiated to the following parameters: a) Power level is enough high, 17 dBm; b) 2 antennas are used c) transmission rate is 3 Mbps. The measurements have been taken several times. Each time the signal was measured at a different location, 10 times in interval of 2–3 minutes. In that way, local interferences such as electrostatic waves, cellular communication and moving objects can be eliminated. At the tested building there is a 51 m corridor with glass and metal doors at the edges. The transmitting and receiving stations were placed on a portable laptop surface. The transmitting accesses point was placed in the beginning of the corridor and at its middle site. Measurements were taken each meter using the laptop. The results of measurements (in dB) with the variance of the average data of 0.5856 are presented in Fig. 6. This

figure shows that with increase of distance between the transmitter and receiver (more than 20–25 m) the effect of attenuation is not sufficient. There are few spikes, which were probably caused by the variance in the walls' architecture characteristics and by some local obstructions such as people walking along corridor.

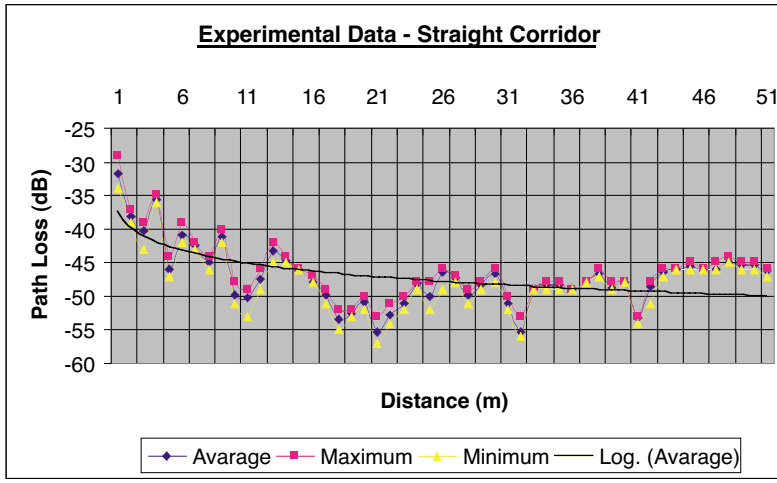

Figure 6. Experimental data along the corridor.

The continues curve in Fig. 6 (according to equation (5)), describe the path loss inside the corridor waveguide, computation of which for the parameters corresponded to this special experiment, for $R_n = 0.7-0.9$, which corresponds to concrete and for $n = 1$ which corresponds to main propagating mode (see the discussion above, after Fig. 4).

Comparison of this result with that obtained theoretically by using equation (5) shows that the mean difference between theoretical prediction and experimental data at the beginning of corridor does not exceed 2–3 dB, becoming of 4–5 dB at its middle sites. It reaches a maximum difference of 9.794 dB at the end of the corridor, where intersection with the crossing corridor exists. So, the corridor waveguide model can be expected as a good predictor of radio coverage inside the straight corridor except some intersections with other crossing corridor within a tested building.

Link Budget for Indoor Links between the Floors and Walls. As above, all the experiments have been carried out in different campuses of the Ben-Gurion University, Israel, each of which is a typical university 3-floor campus, comprising long hallways and contiguous enclosed classrooms with windows. All outside walls are constructed

of concrete. Internal walls are concrete made also. Floors are concrete and covered. There are large windows along the corridors (north wing) and inside every classroom (south wing). Each classroom is furnished with chairs and tables with the same size and heights made from metal and wood. West walls hold teaching boards. During experiments all windows were closed in each floor (both along the corridor and inside each classroom); doors of classrooms remained open and sporadic peoples consumed classes. Measurements were taken between floors. The receiver (Rx) and the transmitter (Tx) were separated with obstructions between them, i.e., having both NLOS and LOS conditions. The transmitter was located in a fixed position at the first floor. The receiver was moved from one location to another location within the measurement area from third floor to the second floor with separation between antennas of two floors and one floor, respectively, and finally at the first floor, the same floor where the transmitter was located.

The proposed model, $L_{total}[\mathrm{dB}] = \overline{L}[\mathrm{dB}] + L_{fading}[\mathrm{dB}]$ is based on the combination of Bertoni's formula of direct penetration through floors and walls (6) and the additional attenuation fading L_{fading}, which takes into account *log-normal* shadowing and multipath effects caused by internal structures and obstructions.

Based on numerous experimental data and measurement analysis, a preliminary suggestion was done that the proposed model predicts the path loss measurements with the smallest deviation from experimental data. In this model L_{fading} values can be found and added by calculating the probability for shadowing, as well as fast fading due to multipath, in the selected area according to receipt described in [2]. Figure 7 presents simulation according to Bertoni's model [described by formulas (6), (8) and (13)] for conditions of experiment described above and the same simulation according to the suggested model (19) with (20)–(23) shown by Fig. 8.

Below we present the distinct difference between the suggested model for predicting path loss between floors (19)–(23) and full Bertoni's path loss prediction model (18), which takes into account diffraction by window corners for the receiver, is at the third floor (Fig. 9) and then the receiver is at the second floor (Fig. 10).

As follows from Fig. 9(a)–(b), the suggested model achieved better agreement with the results of measurements with an average error of 4.76 dB compared with that for Bertoni's model where an average error between prediction and measured data exceeds 10 dB. At the third floor where Rx was located, the term of showing was evaluated to be $L_{fading} = 12.9\,\mathrm{dB}$. At the second floor (see Fig. 10(a)–(b)), the suggested model has again achieved better results with error of 8.00 dB

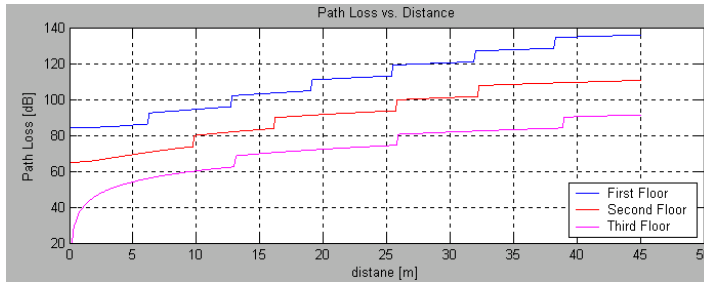

Figure 7. Path Loss obtained from Bertoni's model versus the distance for terminal antennas separated by one, two and three floors.

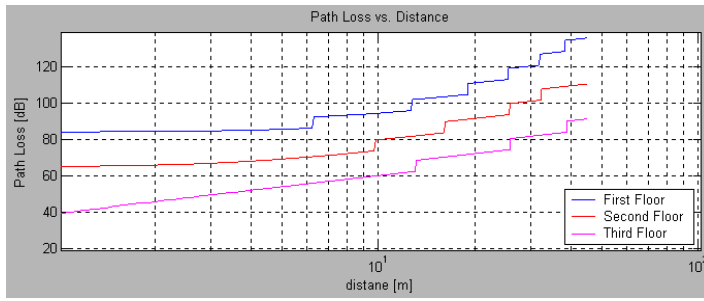

Figure 8. Path Loss obtained from the suggested model versus the distance for terminal antennas separated by one, two and three floors.

compared to error of 9.58 dB obtained from Bertoni's simulation. At the second floor the term of showing was $L_{fading} = 8.1$ dB.

We do not present here results of measurements in a situation when both terminal antennas were located at the same first floor, pointed out a fact that the suggested model achieved better results with an average error of 7.2 dB compared to Bertoni's simulations with error of 8.38 dB. At the first floor the term of showing was evaluated to be $L_{fading} = 6.5$ dB. For numerical computation of total path loss according to Bertoni's model (13) the wall attenuation factor of 4 dB (for concrete walls) and the floor attenuation factor of 13 dB (for mixed concrete walls) were accounted.

The cumulative effect of deviation of theoretical prediction based on suggested model (19)–(23) and measured data carried out for different three-storey building campuses of Ben Gurion University is shown in Fig. 11. According to results presented above, we can conclude that the suggested model is very simple in terms of calculation

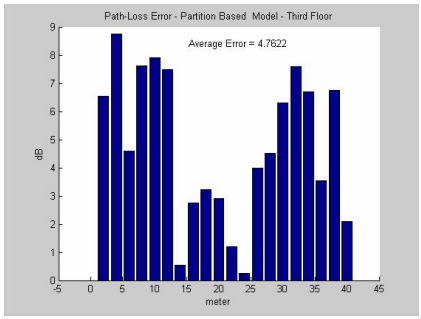

(a)

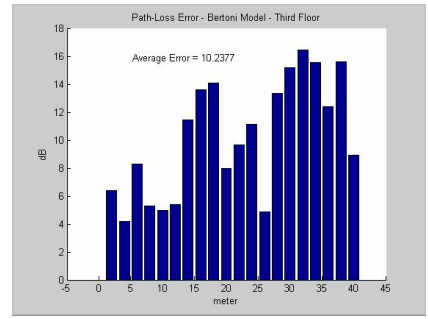

(b)

Figure 9. (a) Error of suggested model compared to measurements. (b) Error of Bertoni's 3rd floor simulation to measurements.

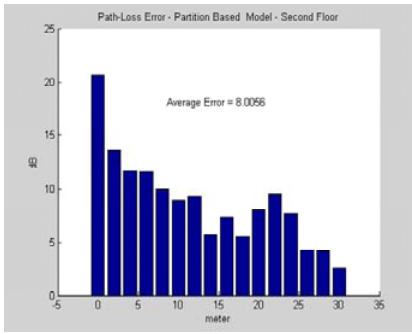

(a)

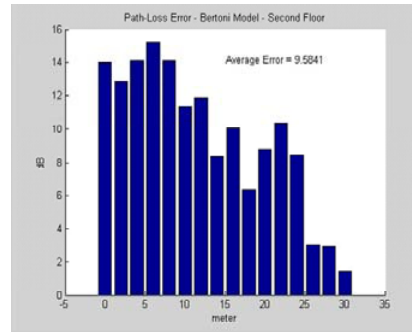

(b)

Figure 10. (a) Error of suggested model compared to measurements. (b) Error of Bertoni's 2nd floor simulation compared to measurements.

and can be easily fit by software to any given indoor experimental site. This model takes into account the *slow* and *fast* fading (statistical approach) unlike other models. At the same time, the proposed model and the corresponding simulation results do not take into account inner objects of rooms and hallways such as: furniture, people and their movements. Therefore, a deviation error was estimated between simulation and link test.

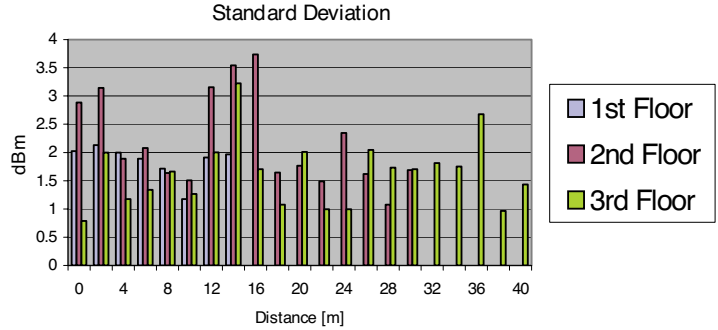

Figure 11. Cumulative effect of error obtained by use the proposed model compared with experimental data.

4. SUMMARY

We can conclude that the suggested model (19)–(23) can be successfully used to predict the total path loss inside buildings for different mutual position of terminal antennas, at the same floor or not. That is if we take into account the strict Bertoni's formulas (6) for the direct path loss between floors and walls and the fading effects, which can be obtained either from experimental data (i.e., parameters σ_L, σ, K) or using method of fading effect estimations described by (19)–(23) following [2], where this approach was successfully used for link budget performance in various outdoor communication links. Comparison with above measurements and the Bertoni's model taking into account both direct loss (6) and diffraction (8) effects in (13) has shown that the proposed semi-empirical approach can be successfully used also for link budget design in various indoor communication links.

REFERENCES

1. Bertoni, H. L., *Radio Propagation for Modern Wireless Systems,* Prentice Hall PTR, New Jersey, 2000.
2. Blaunstein, N., *Wireless Communication Systems, Handbook of Engineering Electromagnetics,* Ch. 12, 417–489, Marcel Dekker, NY, 2004.
3. Rappaport, T. S., *Wireless Communications*, Prentice Hall PTR, New York, 1996.
4. Saunders, S. R., *Antennas and Propagation for Wireless Communication Systems,* J. Wiley & Sons, New York, 1999.

5. Cox, D. C., R. R. Murray, and A. W. Norris, "Measurements of 800 MHz radio transmission into buildings with metallic walls," *AT&T Bell Lab. Tech. J.,* Vol. 62, 2695–2717, 1983.
6. Davidson, A. and C. Hill, "Measurement of building penetration into medium building at 900 and 1500 MHz," *IEEE Trans. Veh. Technol.,* Vol. 46, 161–167, 1997.
7. Turkmani, A. M. D. and A. F. de Toledo, "Modeling of radio transmission into and within multistory buildings at 900, 1800, and 2300 MHz," *IEE Proc.-1,* Vol. 40, 462–470, 1993.
8. Alexander, S. E., "Radio propagation within buildings at 900 MHz," *Electronics Letters,* Vol. 18, No. 21, 913–914, 1982.
9. Hashemi, H., "The indoor radio propagation channel," *Proc. IEEE,* Vol. 81, No. 7, 943–968, 1993.
10. Lemieux, J. F., M. Tanany, and H. M. Hafez, "Experimental evaluation of space/frequency/polarization diversity in the indoor wireless channel," *IEEE Trans. Veh. Technol.,* Vol. 40, No. 3, 569–574, 1991.
11. Rappaport, T. S., "Characterization of UHF multipath radio channels in factory buildings," *IEEE Trans. Antennas Propagat.,* Vol. 37, No. 8, 1058–1069, 1989.
12. Devasirvatham, D. M., M. J. Krain, and T. S. Rappaport, "Radio propagation measurements at 850 MHz, 1.7 GHz, and 4.0 GHz inside two dissimilar office buildings," *Electronics Letters,* Vol. 26, No. 7, 445–447, 1990.
13. Rappaport, T. S. and D. A. Hawbaker, "Wide-band microwave propagation parameters using cellular and linear polarized antennas for indoor wireless channels," *IEEE Trans. on Communications,* Vol. 40, No. 2, 231–242, 1992.
14. Tarng, J. H., W. R. Chang, and B. J. Hsu, "Three-dimensional modeling of 900 MHz and 2.44 GHz radio propagation in corridors," *IEEE Trans. Veh. Technol.,* Vol. 46, 519–526, 1997.
15. Gibson, T. B. and D. C. Jenn, "Prediction and measurements of wall intersection loss," *IEEE Trans. Antennas Propagat.,* Vol. 47, 55–57, 1999.
16. Lafortune, J. F. and M. Lecours, "Measurement and modeling of propagation losses in a building at 900 MHz," *IEEE Trans. Veh. Technol.,* Vol. 39, 101–108, 1990.
17. Arnod, H. W., R. R. Murray, and D. C. Cox, "815 MHz radio attenuation measured within two commercial buildings," *IEEE Trans. Antennas Propagat.,* Vol. 37, 1335–1339, 1989.
18. Whitman, G. M., K. S. Kim, and E. Niver, "A theoretical model

for radio signal attenuation inside buildings," *IEEE Trans. Veh. Technol.,* Vol. 44, 621–629, 1995.

19. Seidel, S. Y. and T. S. Rappaport, "Site-specific propagation prediction for wireless in-building personal communication system design," *IEEE Trans. Veh. Technol.,* Vol. 43, 879–891, 1994.
20. Seidel, S. Y. and T. S. Rappaport, "914 MHz path loss prediction models for indoor wireless communication in multifloored buildings," *IEEE Trans. Antennas Propagat.,* Vol. 40, No. 2, 207–217, 1992.
21. Honcharenko, W., H. L. Bertoni, J. Dailing, J. Qian, and H. D. Lee, "Mechanisms governing UHF propagation on single floors in modern office buildings," *IEEE Trans. Veh. Technol.,* Vol. 41, No. 4, 496–504, 1992.
22. Honcharenko, W., H. L. Bertoni, and J. Dailing, "Mechanisms governing propagation between different floors in buildings," *IEEE Trans. Antennas Propagat.,* Vol. 41, No. 6, 787–790, 1993.
23. Dersch, U. and E. Zollinger, "Propagation mechanisms in microcell and indoor environments," *IEEE Trans. Veh. Technol.,* Vol. 43, 1058–1066, 1994.
24. Clarke, R. H., "A statistical theory of mobile-radio reception," *Bell Systems Technical Journal,* Vol. 47, 957–1000, 1968.
25. Rappaport, T. S. et al., "Statistical channel impulse response models for factory and open plan building communication system design," *IEEE Trans. on Communications,* Vol. 39, No. 5, 794–805, 1991.
26. Devasirvatham, D. M. J., "Time delay spread and signal level measurements of 850 MHz radio waves in building environments," *IEEE Trans. Antennas Propagat.,* Vol. 34, No. 2, 1300–1305, 1986.
27. Rappaport, T. S. and V. Fung, "Simulation of bit error performance of FSK, BPSK, and $\pi/4$-DQPSK in flat fading indoor radio channels using measurement-based channel model," *IEEE Trans. Veh. Technol.,* Vol. 40, No. 4, 731–739, 1991.
28. Kanatas, A. G., I. D. Kountouris, G. B. Kostraras, and P. Constantinou, "A UTD propagation model in urban microcellular environments," *IEEE Trans. Veh. Technol.,* Vol. 46, No. 2, 185–193, 1997.
29. Katedra, M. F., J. Perez, F. S. de Adana, and O. Gutierrez, "Efficient ray-tracing techniques for three-dimensional analyses of propagation in mobile communications: application to picocell and microcell scenarios," *IEEE Antennas Propagat. Magazine,* Vol. 40, No. 2, 15–28, 1998.

30. Kim, S. C., B. J. Guarino, Jr., T. M. Willis, III, et al., "Radio propagation measurements and prediction using three dimensional ray tracing in urban environments at 908 MHz and 1.9 GHz," *IEEE Trans. Veh. Technol.,* Vol. 48, 931–946, 1999.
31. Keenan, J. M. and A. J. Motley, "Radio coverage in buildings," *BT Tech. J.,* Vol. 8, No. 1, 19–24, 1990.
32. "Propagation data and prediction models for the planning of indoor communication systems and local area networks in the frequency range 900 MHz to 100 GHz," International Telecommunication Union, ITU-R Recommendation P. 1238, Geneva, 1997.
33. Blaunstein, N., "Average field attenuation in the non-regular impedance street waveguide," *IEEE Trans. on Antennas Propagation*, Vol. 46, No. 12, 1782–1789, 1998.